

# MODELING OUT-OF-PLANE BEHAVIOR OF URM WALLS RETROFITTED WITH FIBER COMPOSITES

By J. I. Velazquez-Dimas<sup>1</sup> and M. R. Ehsani,<sup>2</sup> Fellow, ASCE

**ABSTRACT:** Although masonry is one of the oldest construction materials, its behavior has not been investigated as extensively as other construction materials. Out-of-plane failures are common in unreinforced masonry (URM) buildings constructed in seismic regions. Seven half-scale brick masonry walls were constructed, externally strengthened with vertical glass fabric composite strips, and subjected to static cyclic out-of-plane loading. The flexural behavior of the tested specimens is characterized by three main stages corresponding to the first visible bed-joint crack, the first delamination, and the ultimate load. The main parameters being investigated in this study are the amount of composite, the height-to-thickness ratio  $h/t$ , the tensile strain in composites, and the mode of failure. Based on the trends observed in the experimental phase, it was concluded that the behavior of the walls is best predicted with a linear elastic approach. It was also concluded that the ultimate strength method overestimates the flexural capacity and the ultimate deflection of the wall. Preliminary design recommendations are also proposed for tensile strain in the composite, maximum deflection, and maximum reinforcement ratio.

## INTRODUCTION

Masonry is one of the oldest construction materials. For thousands of years masonry was the predominant building material until modern materials such as concrete, steel, and wood appeared in the nineteenth century (Abrams 1996). The mechanical properties of masonry are much more complicated than those of other construction materials. For many years, lack of research and understanding of the behavior of masonry led to reluctance by the engineering community in widespread use of this material. However, a large number of research projects conducted on masonry in the last 20 years have demonstrated the feasibility of this material for many applications. As a result, masonry seems to be returning as a reliable construction alternative. Most of the recent research has focused on improving the seismic safety of new buildings being constructed with masonry.

Unreinforced masonry (URM) buildings constitute a significant part of the existing building inventory worldwide. URM buildings are vulnerable to lateral loads such as those caused by earthquakes or high speed winds. In the event of an earthquake, these lateral forces are transferred to the foundation through load-bearing walls. These structural elements may be subjected to in-plane or out-of-plane loads. Failure in URM buildings due to out-of-plane loads is considered the main cause of personal injury and loss of life during earthquakes.

Recognizing the shortcomings of URM buildings, there has been a surge of interest in recent years to develop techniques for improving seismic behavior of these structures. A number of techniques have been proposed, and a complete overview of these approaches has been documented by Lizundia et al. (1997). Among the new techniques for seismic retrofit of URM buildings is the patented process of thin sheets of fiber composites to the wall surface [M. R. Ehsani and H. Saadatmanesh, "Method of strengthening masonry and concrete walls with composite strap and high strength random fibers," U.S. Patent No. 5,640,825 (1997)]. Recent field applications have demonstrated the feasibility of this procedure (Ehsani and Saadatmanesh 1996, 1997).

<sup>1</sup>Prof. of Civ. Engrg., Autonomous Univ. of Sinaloa, Mexico CP80000.

<sup>2</sup>Prof. of Civ. Engrg. and Engrg. Mech., University of Arizona, Tucson, AZ 85721. E-mail: ehsani@u.arizona.edu

Note. Discussion open until April 1, 2001. To extend the closing date one month, a written request must be filed with the ASCE Manager of Journals. The manuscript for this paper was submitted for review and possible publication on October 14, 1998. This paper is part of the *Journal of Composites for Construction*, Vol. 4, No. 4, November, 2000. ©ASCE, ISSN 1090-0268/00/0004-0172-0181/\$8.00 + \$.50 per page. Paper No. 19440.

## SCOPE OF WORK

This paper describes different methodologies for modeling the behavior of URM masonry walls retrofitted with glass-fiber composites and subjected to cyclic out-of-plane loading. The proposed method is based on experimental data generated through seven tested URM walls. The data analyzed included several design parameters such as the amount of reinforcement and height-to-thickness ratio  $h/t$  as well as the observed behavior in terms of modes of failure, maximum measured longitudinal strains in composite strips, compressive strain in brickwork, and out-of-plane deflection. The behavior of the walls is represented through three main stages associated with the loss of flexural stiffness of the walls, which are the formation of the first visible bed-joint crack, the first delamination, and the mode of failure.

Based on the trends given by the experimental data, a methodology for estimating the ultimate flexure capacity of the walls is proposed. In addition, equations for calculating the deflections at first visible bed-joint crack and at formation of the first delamination are presented that take into account the height-to-thickness ratio of the walls. The proposed method is valid for walls that are simply supported at the top and bottom and are free along the other two sides. These boundary conditions are representative of midsections of walls away from corners. In light of the limitations of the experimental program, additional studies are needed before the findings can be generalized. Such studies could investigate the effects of different types of fibers (e.g., carbon and aramid), different boundary conditions, number of wythes of brick in the wall, and brick surface conditions.

## PREVIOUS STUDIES

A number of analytical procedures have been proposed for evaluation of the behavior of masonry walls subjected to out-of-plane loading. Some of the proposed methodologies are based on classical mechanics of materials, elastic plate theory, and finite-element method. Some of these methods have been reformulated in order to estimate the ultimate flexural capacity of URM panels. These modifications consider the yield line theory and the fracture line theory. Most of these methods are applicable to infill panels with different boundary conditions.

Sinha (1978) proposed a simplified method based on fracture lines that could be applied to any brittle material having strength and stiffness orthotropy. His proposed method correlated very well with the experimental results. In that study, many panels with different boundary conditions were ana-

lyzed, and a theoretical formulation for the collapse load was proposed for each panel considering the support conditions and the aspect ratio.

Dawe et al. (1988), conducted an extensive parametric study on hollow concrete block infill panels subjected to out-of-plane loading. The main parameters considered were panel thickness, infill strength, boundary conditions, frame rigidity, and geometric aspect ratios. Based on the results of this study, empirical relations suitable for design were proposed. Arching action and yield line analysis were also incorporated into the proposed method. It was concluded that the ultimate load increases parabolically when panel thickness is increased and decreases when the length and height of the panel are increased.

Sveinsson et al. (1987) developed an analytical model for steel-reinforced block masonry walls subjected to out-of-plane seismic motions. In the model, three linear stages were proposed representing the following ranges of loading: before cracking, between cracking and yielding, and postyield. Three elements were incorporated in the model for cyclic behavior for the investigated walls: two face shells, a steel-reinforcing bar across the joint, and an elastic masonry block between the joints. Face shell elements were assumed to have no tension capacity and to behave elastically in compression. The steel bar was modeled by a bilinear stress-strain curve. To validate the proposed analytical model, three full-scale reinforced concrete block masonry walls were constructed. The specimens were tested under simulated seismic input motions applied by two servocontrolled hydraulic jacks located at the top and bottom. Comparing the results, Sveinsson et al. concluded that the analytical model predicted the overall response of the tested walls very well.

Abrams et al. (1993), conducted an experimental and analytical study to evaluate the flexural capacity of infill panels previously tested under in-plane loading. These results were compared with predictions given by analytical models developed by several researchers. The best predictions were given by models taking into account either fracture line theory or yield line theory. They found that the panel strength is inversely proportional to the square of the height-to-thickness ratio. It was also concluded that significant arching action develops for panels with  $h/t < 20$ . For slender panels, the capacity is controlled by flexure.

As noted above, very little information is available in the literature for walls that are simply supported at the top and bottom. In particular, no studies were found on predicting the behavior of URM panels retrofitted with composite overlays.

## FIBER COMPOSITE MATERIALS

Composite materials consist of strong fibers such as carbon, glass, and aramid bound together by a matrix. The matrix can be vinyl ester, polyester, or epoxy resin. Composite materials have been used for more than 40 years in the aerospace industry and other industries. The mechanical properties of composite materials depend on the fiber-to-matrix ratio. In composite materials, the fibers provide strength and stiffness to satisfy design requirements, and the matrix provides load transfer among fibers, dimensional stability, and fiber support and protection. Composite materials have many advantages over conventional materials such as steel. Among them are high specific strength, high specific stiffness, noncorrosiveness, high fatigue resistance, thermal stability, low cost, and ease of installation. By selecting the appropriate fiber, matrix, and geometry, composite materials can be tailored to satisfy a specific application. They also present some disadvantages such as low in-plane transverse (i.e., shear) strength, low interlaminar strength, linear elastic behavior up to failure, and

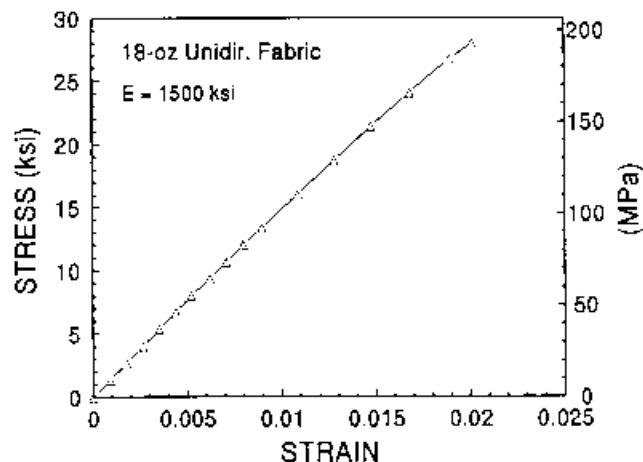


FIG. 1. Stress versus Strain for Unidirectional Glass Composite

potential sensitivity to moisture and UV radiation (Jones et al. 1975; Madenci 1997).

The advantages of composite materials make them an ideal material for construction applications. To manufacture composite products, many procedures can be used such as filament winding, pultrusion, compression molding, and hand layup. Many composite products for civil engineering projects are available in the form of structural shapes; reinforcing bars and tendons for concrete structures; fabrics for retrofitting beams, columns, walls, etc. In the last 10 years, many research and field applications on composite materials have been reported (Nanni 1993; Taerwe 1995; El-Badry 1996; Saadatmanesh and Ehsani 1996, 1998).

The fibers have very high tensile strength, typically exceeding that of metals. For construction applications, usually more than 40% of the total volume of the composite products is the resin matrix whose contribution to the strength or stiffness of the composite is minimal. For the retrofit of masonry walls reported here, a unidirectional glass fabric weighing  $610 \text{ g/m}^2$  (18 ounces/square yard) and a two-component epoxy matrix was used. The hand layup technique used to apply the fabric to the wall resulted in a resin-rich composite. Fig. 1 shows a typical stress versus strain curve for the composite used in this study. The stresses are calculated based on gross cross section according to ASTM D 3039.

## DISCUSSION OF EXPERIMENTAL RESULTS

The experimental data analyzed in this paper were obtained from seven half-scale URM walls constructed with solid clay bricks and a low strength mortar. The specimens were divided into two sets: the short walls [710 mm (28 in.) high] and the slender walls [1,420 mm (56 in.) high] with a height-to-thickness ratio of 14 and 28, respectively. All specimens were 1,220 mm (48 in.) wide. Each wall was designated with a letter followed by one or two numbers. The letter "S" refers to single wythe and the letter "D" to double wythe. The designation for "S" series specimens is followed by two numbers that refer to the percentage of the composite reinforcement on the south and the north faces of the wall with respect to the balanced condition, respectively. A number indicating the reinforcement ratio for the north face follows the letter "D." The balanced reinforcement ratio was calculated similar to that for reinforced concrete members, assuming that masonry fails in compression at a strain of 0.003 at the same time that the composite fails in tension at a strain of 0.02.

All materials (sand, brick units, mortar, and composites) and brickwork assemblages were characterized according to the appropriate ASTM standards. Thus, the compressive capacity

of brick units was 45 MPa (6.52 ksi) and the mortar compressive strength was 5,190 kPa (754 psi) at 28 days, and 7,200 kPa (1,044 psi) at testing time. The half-scale brick units were assembled together with a 6 mm (0.25 in.) wide mortar bed-joint constructed of sand passing mesh No. 18. From prisms constructed with five bricks, the compression capacity of brickwork was determined as 20.0 MPa (2.90 ksi) at 28 days and 26.7 MPa (3.87 ksi) at testing time. The modulus of rupture was obtained from brick beam tests as 1,482 kPa (215 psi) at 28 days and 1,613 kPa (234 psi) at testing time. Finally, the unidirectional glass fiber used for retrofitting the specimens was tested in pure tension, and its tensile strength was 369 N/mm (2,106 lb/in.) width of fabric.

All specimens were subjected to the same standard history pattern of static cyclic out-of-plane loading applied with an air-bag system that was moved from one face of the wall to the other. The load was applied to the wall faces in two stages: (1) A load-controlled stage, which consisted of two pairs of cycles to observe the uncracked behavior; and (2) a displacement-controlled stage, where the maximum displacement in each pair of cycles remained constant. The stiffness degradation was monitored using two loading cycles for the same displacement level. No axial load was applied to the specimens

to exclude the beneficial effects of overburden stress. The specimens were simply supported at the top and bottom and remained free along the vertical edges. A roller condition was also provided at the top (i.e., vertical displacements and rotations were allowed). With these boundary conditions, it was intended to reproduce a portion of the wall free of corner and joint interference.

Fig. 2 shows a general overview of the test setup. Experimental results and material properties of all specimens are discussed elsewhere (Velazquez-Dimas 1998; Ehsani et al. 1999). The main parameters investigated in this study are summarized in Table 1. In addition, the load versus deflection envelopes for all load histories are shown in Fig. 3. From these graphs, it can be seen that the flexural capacity and ductility of URM walls retrofitted with glass-fabric composites are significantly enhanced. For example, some of the tested specimens deflected to drift levels of 5%, supported more than 30 times their aerial weight and resisted a large number of loading cycles.

The midheight deflection corresponding to the formation of the first delamination for the specimens are as follows: S20, 7 mm; S25, 5 mm; S30, 6 mm; S40, 10 mm; S75, 8 mm; S50, 21 mm; D100, 20 mm; S100, 25 mm; S200, 33 mm; and S300, 25 mm.

Because delamination controlled the mode of failure of the majority of the tested specimens, longitudinal tensile strain in composite strips, deflections at midheight, and the reinforcement ratio are considered to be the most representative parameters for the purposes of this study. For each specimen, the peak tensile strains in the composite strip at midheight of the wall and the average of the three strips at the same location were analyzed. Although each specimen was subjected to a large number of loading cycles, the above strain values were only examined for loads corresponding to the first visible bed-joint crack, the first delamination of the composite strip, and the ultimate failure. According to the observed behavior, these three stages are sufficient to characterize the overall behavior of the tested walls. These results are shown in Figs. 4 and 5. Due to the sudden failure of Specimen S300/300, no data were collected for the tensile strain in the composite at failure.

The experimental data summarized in Fig. 4 and 5 were used to select strain values that would correspond to the different stages of the behavior of the walls. The following values were selected based on judgment, but they are fairly close to the average values reported in those figures. These strain limits are conservative values for predicting the behavior of the retrofitted walls. A longitudinal strain of 0.004 is assumed to occur in composite strips when the first visible bed-joint crack appears. For the first delamination, a longitudinal tensile strain

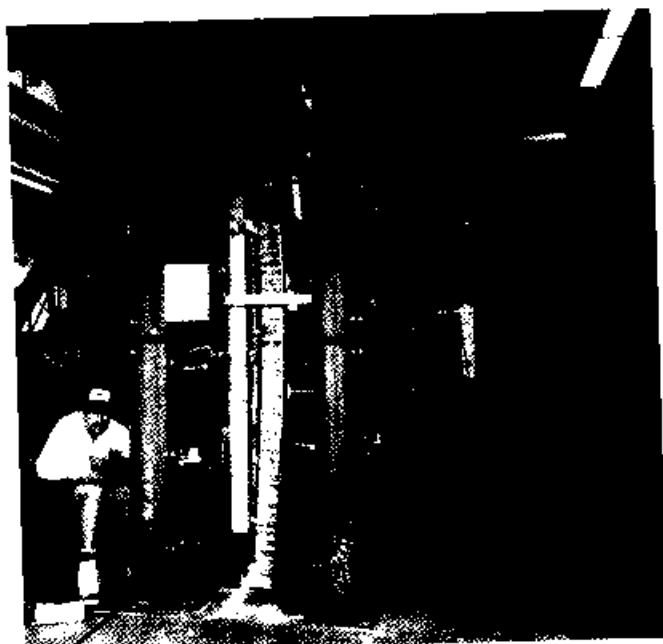


FIG. 2. Test Setup

TABLE 1. Measured Parameters for Tested Specimens

Specimen (1)	h/t (2)	Face (3)	$\rho/\rho_b$ (4)	$P_{max}$ [kPa (psf)] (5)	$\delta_{max}$ [mm (in.)] (6)	Drift (%) (7)	$P_{max}/Wt$ (8)	W [mm (in.)] (9)	Fracture ductility index (10)	Mode of failure (11)	$\epsilon_{max}(t)$ (%) (12)
S75/25	14	North	0.75	31.0 (648)	15.5 (0.6)	2.5	33	102 (4.0)	4.0	D	1.2
	14	South	0.25	12.4 (259)	16.0 (0.63)	2.25	13	34 (1.32)	4.3	D	1.0
S20/40	14	North	0.2	10.3 (216)	12.5 (0.5)	1.8	11	26 (1.06)	5.0	D	1.2
	14	South	0.4	18.6 (389)	5.2 (0.6)	2.1	20	52 (2.12)	3.75	D	1.0
S30/30	14	North	0.3	15.5 (331)	1.25 (0.35)	1.25	16	81 (3.18) <sup>a</sup>	3.5	PD	0.7
	14	South	0.3	16.6 (346)	1.42 (0.4)	1.42	17	81 (3.18) <sup>a</sup>	2.7	T	1.0
S100/100	28	North	1.0	11.7 (245)	4.0 (2.3)	4.0	13	135 (5.3)	4.6	T, D	1.0
	28	South	1.0	11.7 (245)	4.0 (2.3)	4.0	13	135 (5.3)	4.6	D	0.9
S300/300	28	North	3.0	16.7 (350)	2.0 (1.0)	2.0	17.5	406 (16.0)	1.8	NF	0.5
	28	South	3.0	22.7 (475)	2.3 (1.3)	2.3	24	406 (16.0)	2.6	S	0.3
S200/50	28	North	2.0	20.7 (432)	5.0 (2.75)	5.0	23	269 (10.6)	5.0	D, C	1.1
	28	South	0.5	6.2 (130)	3.4 (1.84)	3.4	7	66 (2.6)	4.6	T	1.3
D100	28	North	1.0	9.8 (205)	2.77 (3.0)	2.77	5	279 (11.0)	5.0	D	0.8

<sup>a</sup>Wall was retrofitted with 18-ounce Cross-ply E-Glass fabric.

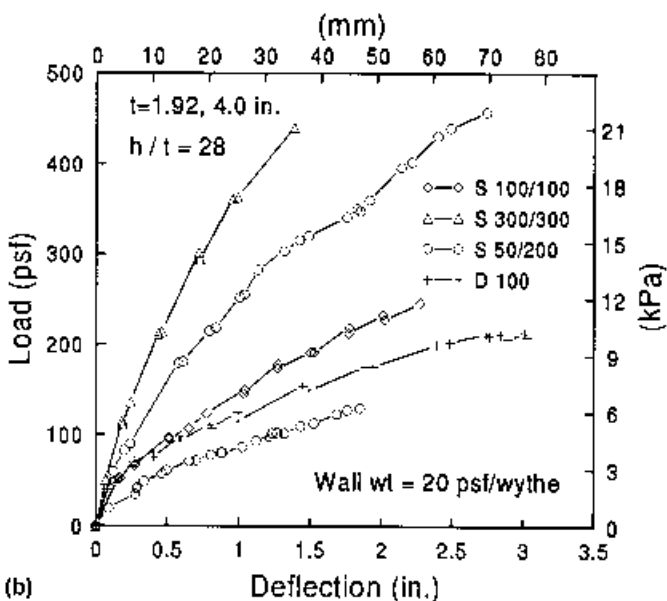
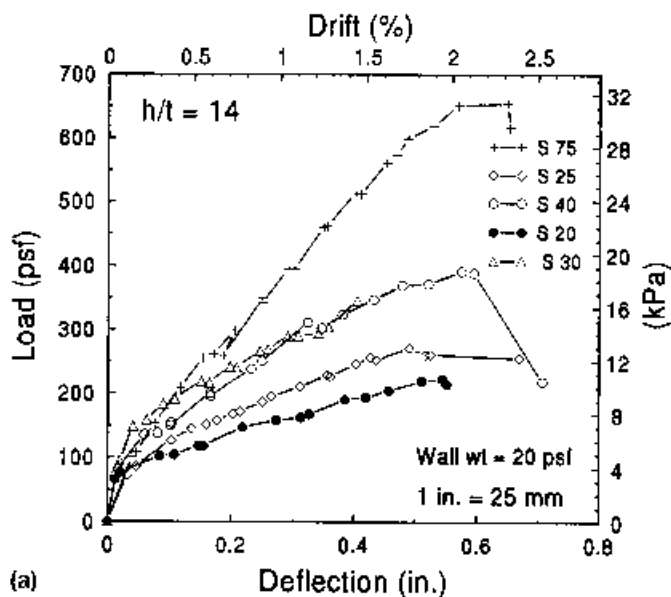


FIG. 3. Load versus Deflection Envelopes: (a) Short Walls; (b) Slender Walls

in the composite strips of 0.0055 is considered. Finally, a tensile strain of 0.01 is assumed for the ultimate failure of the walls. It is noted that based on coupon tests of the composite laminates under pure tension, the failure strain should reach approximately 0.02 (Fig. 1). However, the specimens that failed in tension (mode of failure "T" in Table 1) reached a maximum tensile strain in the composite ranging from 1.0 to 1.3%. This difference is attributed to several factors including the cyclic tension/compression nature of the loading, and the uneven surface of the brick walls. The above values could be used for analytical prediction of the corresponding loading condition. It is important to keep in mind that these values are for URM walls retrofitted with glass-fiber composites only, and therefore more experimental work is needed in order to suggest similar strain values for other fibers such as carbon and aramid.

Midspan deflections for the walls at different stages of loading are summarized in Fig. 6. The calculated points shown in this figure will be discussed later. Experimental data for the short walls indicate that no particular trend exists between the deflection and reinforcement ratio. However, for the slender

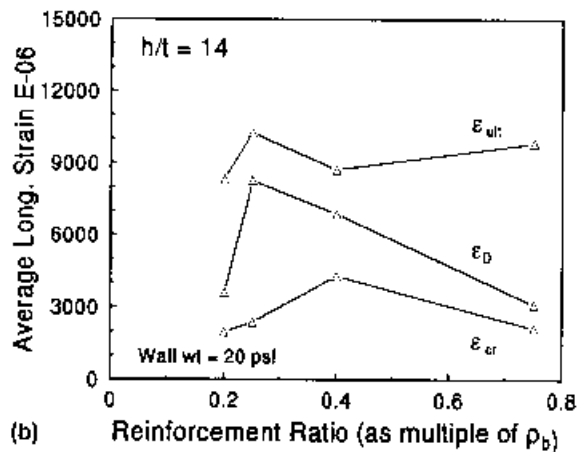
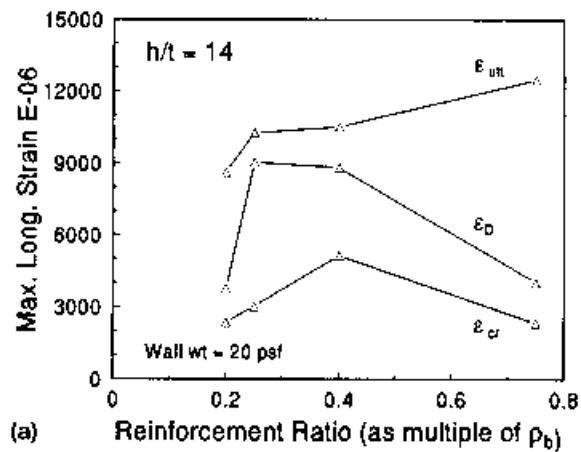


FIG. 4. Strain versus Reinforcement Ratio for Short Walls: (a) Maximum Strain; (b) Average Maximum Strain

walls, there is an increase in deflection as the reinforcement ratio is increased up to two times the balanced condition. The only exception is Specimen S300/300, which failed prematurely due to in-plane shear at the support. Thus this specimen did not experience the degree of delamination that was observed in the remaining specimens.

Fig. 7 shows a dimensionless representation of the load versus the amount of reinforcement in the walls. The applied pressures have been normalized with respect to the weight of the wall. The abscissa depicts the width of the composite strips normalized with respect to the wall thickness. For all stages of loading (i.e., cracking, delamination, and ultimate), there is a nearly linear increase in load with respect to the amount of reinforcement. This is particularly true if the behavior of Specimen S300 ( $W/t = 8.3$ ), which failed by in-plane shear in the wall, is excluded.

## PREDICTION OF OBSERVED BEHAVIOR

The observed experimental results were compared with the predicted values following the ultimate strength method and the linear elastic approach.

### Ultimate Strength Approach

A common method for predicting the flexural capacity of structural elements is the use of the ultimate strength conditions. These calculations require the limit-state conditions for the brick and composite laminate. An ultimate compressive strain of 0.003 was assumed for the masonry. Based on coupon tests, an ultimate tensile strain of 0.02 was selected for the composite materials. To predict the load versus deflection re-

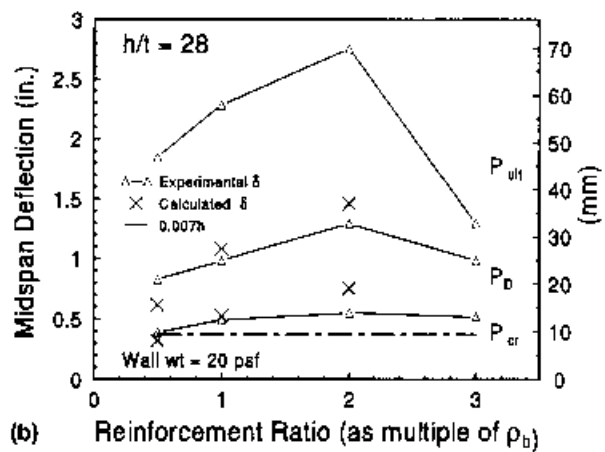
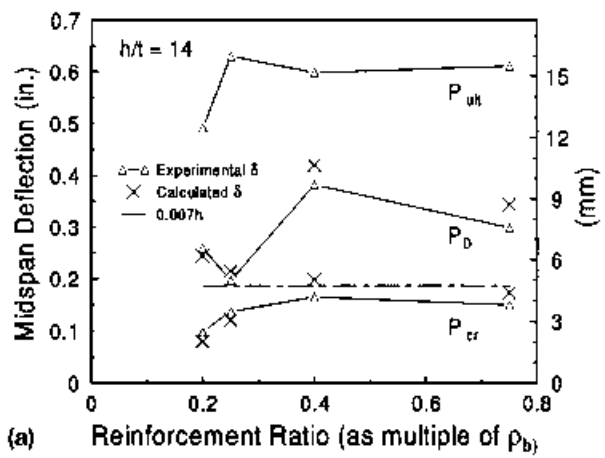
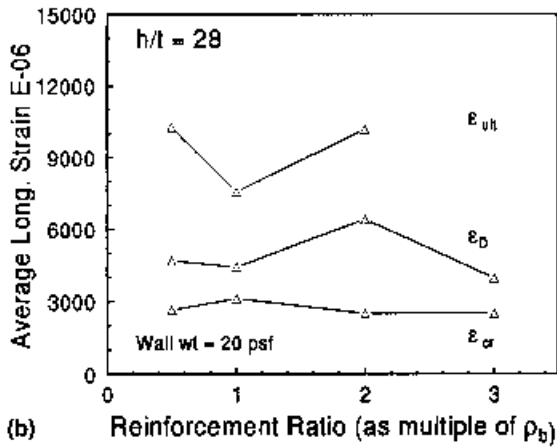
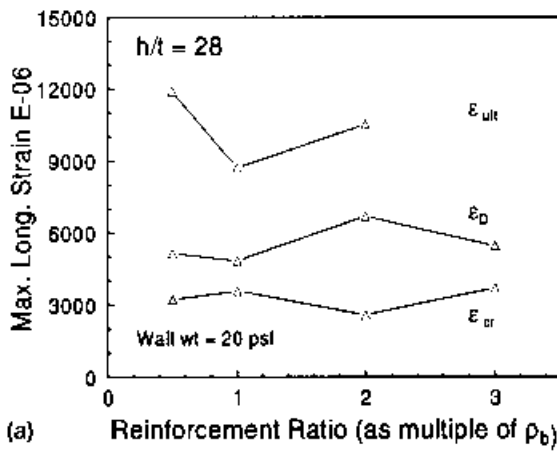


FIG. 5. Strain versus Reinforcement Ratio for Slender Walls: (a) Maximum Strain; (b) Average Maximum Strain

FIG. 6. Midspan Deflection versus Reinforcement Ratio: (a) Short Walls; (b) Slender Walls

sponse of the specimens, a computer program developed for RC beams was modified and then used in this study (Marine 1994).

Results for short and slender specimens are presented in Fig. 8. It is clear that the results calculated based on the ultimate strength approach overestimate the measured experimental values especially for the ultimate load and the maximum deflection. A similar trend was observed for all specimens. The overestimation of the ultimate strength method is attributed to several factors. First, the analysis assumes full composite action between the composite strips and the masonry. However as delamination begins, this assumption is no longer valid. This delamination prevented two modes of failures to take place: (1) Compression failure in the slender walls with high reinforcement ratios; and (2) tensile failure in the short walls with small reinforcement ratios. The second factor contributing to the mismatch of the results is the softening of the brickwork as a result of cyclic loading. Based on these results, the use of the ultimate strength approach is not recommended for estimating the flexural capacity of URM walls retrofitted with composite materials.

### Linear Elastic Approach

Considering the observed behavior of the tested specimens, where the mode of failure was controlled by delamination, it was decided to estimate the flexural capacity using a linear elastic approach. The use of such an approach can be justified because none of the tested specimens failed by compression crushing of the brick. Weak interface between the composite strips and the surface of the brickwork, caused by the large number of loading cycles, resulted in excessive delamination

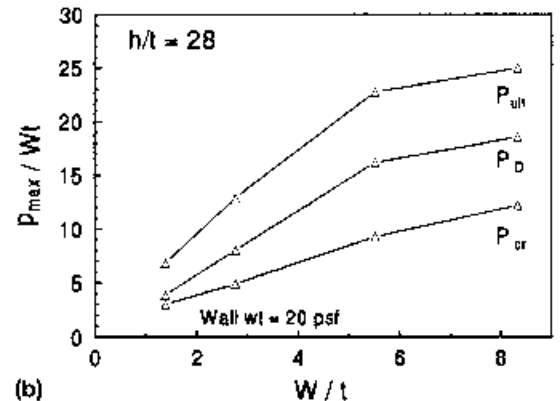
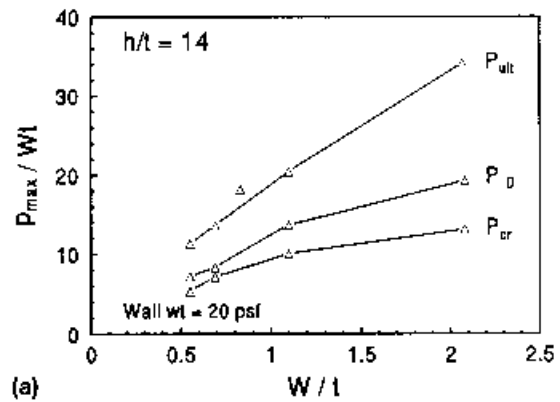
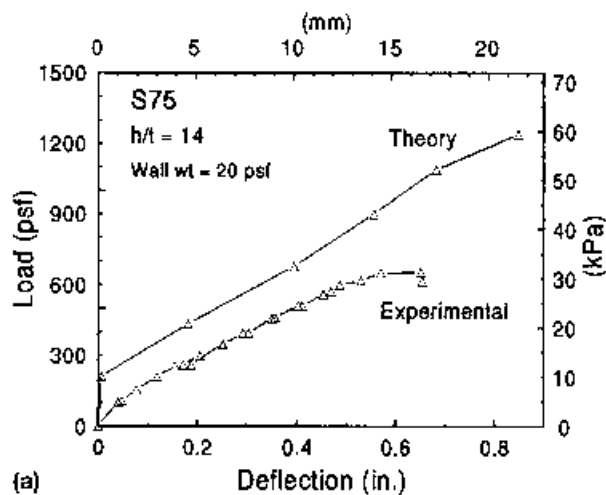
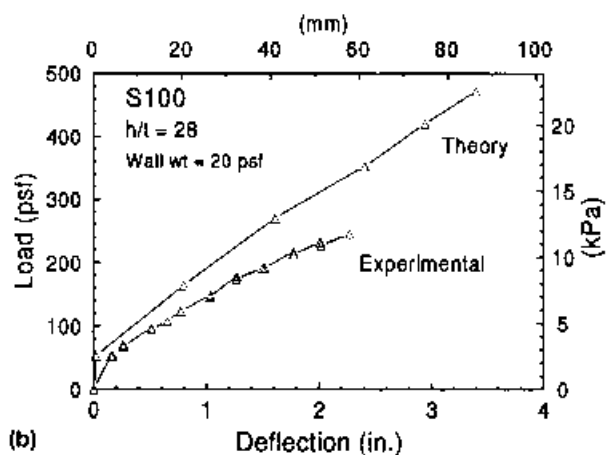


FIG. 7. Normalized Pressure versus Width of Composite Strip: (a) Short Walls; (b) Slender Walls



(a)



(b)

FIG. 8. Theoretical and Experimental Load versus Midspan Deflection: (a) Specimen S75; (b) Specimen S100

that eliminated the possibility of compression failure of brick. Therefore, both materials (i.e., the composite strips and the brickwork) can be assumed to behave linearly elastic for the entire loading history.

The theoretical load corresponding to the three stages of loading for each specimen (i.e., the first visible bed-joint crack, the first delamination, and the ultimate condition) was calculated assuming linear elastic behavior. The analysis for the first visible bed-joint crack was carried out assuming a tensile strain in the composite strip of 0.004. To calculate the load corresponding to the formation of the first delamination, a tensile strain of 0.0055 was considered. In addition, a tensile strain of 1% was assumed to obtain the ultimate load; this conservative value is justified since tensile failure was reached at this strain level (Table 1). Furthermore, the tensile strength of brickwork was neglected, and the analysis was carried out on transformed sections. Using the above tensile strains in the composite strips, the compressive strains and stresses in the brick were calculated by a trial-and-error procedure such that equilibrium of forces would be satisfied.

The *Uniform Building Code* (UBC) [International Conference of Building Officials (ICBO) 1991] limits the service load deflection of steel reinforced masonry walls to 0.7% of the wall height (i.e., UBC Eq. 11-10)

$$\delta_s \leq 0.007h \quad (1)$$

For the tested specimens, this limit has been calculated and the results are shown as dashed lines in Fig. 6. It is clear that the above serviceability limit state is very close to the deflections that correspond to the observation of the first bed-joint

cracks. In all cases, the specimens had significant reserve capacity in terms of load and deflection beyond this limit. It can therefore be concluded that the same limit can be considered for URM walls that have been retrofitted with externally bonded composite strips.

The UBC also recommends Eqs. 11-11 and 11-12 for calculating the midheight deflections of walls as given below

$$\delta_s = \frac{5Mh^2}{48E_m I_g} \quad (\text{for } M \leq M_{cr}) \quad (2)$$

$$\delta_s = \frac{5M_{cr}h^2}{48E_m I_g} + \frac{5(M_{ser} - M_{cr})h^2}{48E_m I_{cr}} \quad (\text{for } M_{cr} < M \leq M_{cr}) \quad (3)$$

Analysis of the data revealed that the use of the above equations would underestimate the measured deflections of the test specimens. It is believed that the complex behavior of masonry walls due to the nonhomogeneous and orthotropic nature of the brick masonry and the presence of the composite strips cannot be adequately accounted for by the above equations. The data also indicated that, although the above equations underestimated the deflections for short and slender walls, the discrepancy between the equations and the test results was nearly twice as high for specimens with  $h/t = 14$ . It is recognized that, because the thickness of the specimens was the same, this behavior could be attributed to the variation in  $h/t$  or  $h$ . However, it was decided to modify the equations assuming that this discrepancy was due to  $h/t$  rather than  $h$ . Additional data are needed to examine the validity of this assumption.

Therefore, a modification of the above equations in the forms presented below is suggested to account for the observed behavior of the walls. To calculate the midspan deflections for service moments smaller than that for cracking (i.e.,  $M \leq M_{cr}$ ), (2) can be modified as follows:

$$\delta_s = \frac{6Mh^2}{\left(\frac{h}{t}\right) E_m I_g} \quad (4)$$

To calculate the deflection when the first visible bed-joint crack occurs (i.e., when  $M_{cr} < M < M_{cr}$ ), (3) is modified as follows:

$$\delta_{ser} = \frac{6M_{cr}h^2}{\left(\frac{h}{t}\right) E_m I_g} + \frac{2(M_{ser} - M_{cr})h^2}{\left(\frac{h}{t}\right) E_m I_{cr}} \quad (5)$$

where

$$M_{cr} = \frac{f_c I_g}{\left(\frac{h}{t}\right)} \quad (6)$$

To calculate the deflection when the service moment is smaller than that for the first delamination but larger than for the first visible bed-joint crack (i.e.,  $M_{cr} < M < M_{cr}$ ), the following equation is recommended:

$$\delta_s = \delta_{ser} + \frac{2.5(M_{ser} - M_{cr})h^2}{\left(\frac{h}{t}\right) E_m I_{cr}} \quad (7)$$

The flexural moments  $M_{cr}$  and  $M_{cr}$  correspond to tensile strain of the composite equal to 0.004 and 0.0055, respectively, and can be calculated using the conventional approach used for reinforced concrete beams whereby a depth to the neutral axis satisfying equilibrium is determined. For all test specimens, the load was calculated for the three stages of loading. The corresponding deflections were also calculated according

to the above procedures; however, the deflections were calculated for the cracking and delamination points only. No deflections were calculated for the ultimate condition due to the complex failure mechanisms observed on all walls. These calculated loads and deflections are shown in Fig. 9. In these calculations, the measured modulus of elasticity of the brickwork, which was 4,530 MPa (657 ksi), was used. This value is considerably lower than the recommended value of  $E_w = 750f'_m$  (ICBO 1991); the latter would result in a modulus of 14,890 MPa (2,160 ksi) for the tested specimens.

As stated earlier, because the ultimate deflections were not calculated, the ultimate point for each of the calculated graphs in Fig. 9 could not be shown. However, the loads for these ultimate points were calculated, and they were in very good agreement with the measured results. The calculated ultimate loads and the corresponding experimental value for all specimens are listed in Table 2. The results indicate that the linear

**TABLE 2. Experimental and Calculated Ultimate Load for Tested Specimens**

Specimen (1)	h/t (2)	$\rho/\rho_b$ (3)	P [kPa (psf)]		Error (%) (6)
			Experimental (4)	Calculated (5)	
S20/40	14	0.2	10.3 (216)	9.24 (193)	+12.0
	14	0.4	18.6 (389)	18.34 (383)	+1.6
S75/25	14	0.75	11.7 (248)	14.33 (297)	-9.6
S100/100	28	1.0	11.7 (245)	11.3 (236)	+3.8
S200/50	28	2.0	20.7 (432)	22.31 (466)	-7.3
	28	0.5	6.2 (130)	5.7 (119)	+9.2
S300/300	28	3.0	22.7 (475)	33.37 (697)	-32.0

elastic approach gives a better prediction of the flexural capacity of URM walls retrofitted with composite materials. With the exception of Specimen S300, the average difference between the measured and calculated failure loads was <10%.

## DISCUSSION AND PROPOSED ANALYTICAL METHOD

Two methodologies were used to model the behavior of URM walls retrofitted with glass-fiber composite strips. The procedure based on the ultimate strength condition overestimates the flexural capacity of the specimens. Because the materials that comprise the wall (i.e., brickwork and composite strips) behave in a brittle manner, an upper-bound solution is not recommended. Instead, an easier and more conservative analytical method is recommended for modeling the behavior of URM clay brick masonry walls retrofitted with composites. With this alternative, it is intended to incorporate a more realistic behavior of the walls by assuming that they behave linearly elastic up to failure. This is supported by the observed behavior of all specimens, where most of them failed due to excessive delamination after a large number of loading cycles.

To calculate the flexural capacity of retrofitted URM masonry walls using an elastic analysis, the following assumptions were made:

- Plane sections remain plane.
- Tensile strength in brickwork is neglected.
- Linear stress and strain distribution across the wall section is assumed (Fig. 10).
- Full composite action between composite strip and the brick surface is assumed (i.e., strain compatibility is satisfied).
- All compressive forces are resisted by brickwork; the compressive capacity of composite strips is ignored.
- Composite strips take all tensile force in the cross section.
- The mode of failure can be either tensile rupture of composite strips or excessive delamination. No compressive failure of masonry is expected.
- The maximum expected tensile strain in composite strips is 1%.
- Modulus of elasticity of brickwork is calculated as  $E_w = 750f'_m$  (ICBO 1991).

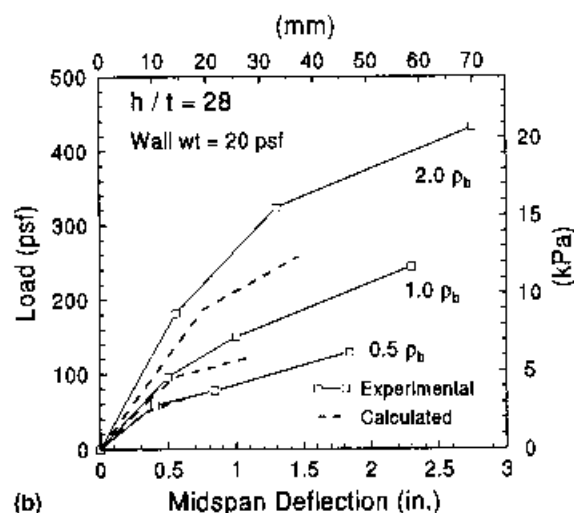
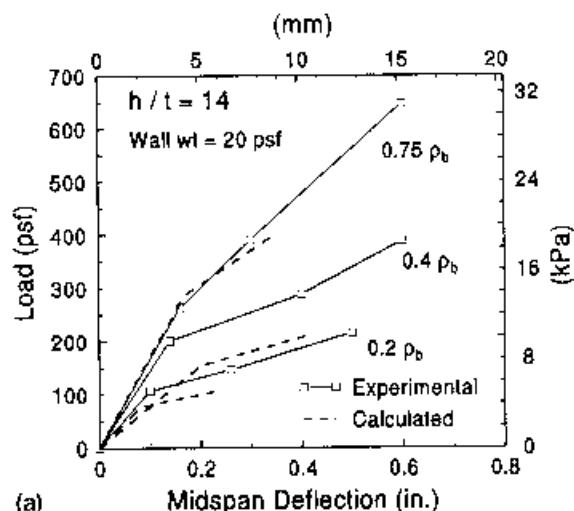


**FIG. 9. Calculated (Elastic Analysis) and Experimental Load versus Midspan Deflection: (a) Short Walls; (b) Slender Walls**

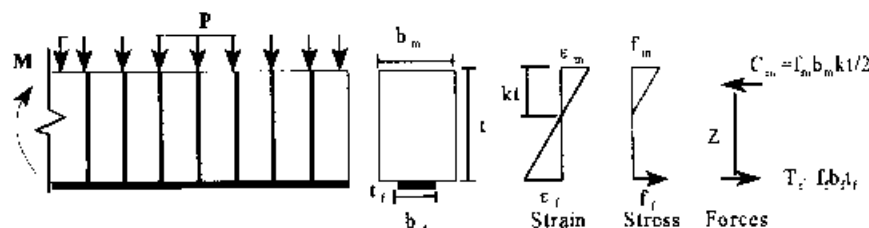


**FIG. 10. Strains, Stresses, and Internal Forces in Brick Masonry Beam**

As stated earlier, the calculation of deflections are very sensitive to the modulus of elasticity of the masonry, and therefore the actual measured modulus was used. However, the effect of modulus of elasticity of the brickwork on the flexural capacity is minimal. Therefore, for these calculations,  $E_m = 750f'_m$  was assumed. Taking summation of moments of the internal stress resultants in Fig. 10, the moment can be calculated as follows:

$$M = T_c Z = f_t W_t Z \quad (8)$$

where  $f_t = E_t \epsilon_t$ ; and  $Z = t - kt/3$ . Substituting for  $Z$  in (8), one obtains

$$M = T_c Z = f_t W_t t \left(1 - \frac{k}{3}\right) \quad (9)$$

Due to the small thickness of the composite laminate, its influence on the moment arms in the above expression has been ignored. For an assumed value of strain in the composite strip, the internal tensile and compressive force resultants can be set equal to one another to obtain the depth of the neutral axis. From this condition, the factor  $k$  can be obtained

$$k = \frac{2f_t W_t}{f_m b_m t} \quad (10)$$

The moment capacity of the wall can be calculated by combining (9) and (10).

## PRELIMINARY DESIGN RECOMMENDATIONS

The writers recognize that this is the first reported investigation on a study of the behavior of URM retrofitted with fiber composites. Considering the scope of this study, it is evident that additional investigations are required before a set of comprehensive design guidelines can be established. However, based on the observed behavior of the specimens and the analysis of the results, the following preliminary design recommendations are provided.

### Reinforcement Ratio

For the specimens with  $h/t = 14$ , the maximum reinforcement ratio tested was  $0.75\rho_p$ . The failure of this specimen was rather explosive due to the high pressure applied to the wall at failure. On the other hand, the specimen with a reinforcement ratio of  $0.4\rho_p$  exhibited a more ductile failure and deformed to the same ultimate deflection. Therefore, it is recommended that, for walls having an aspect ratio of 14, the reinforcement ratio be limited to  $0.4\rho_p$ .

For walls with an aspect ratio of 28, the highest tested reinforcement ratio was  $3\rho_p$ . This specimen failed by in-plane shear failure of the brickwork and showed a very stiff behavior. Based on the observed behavior of this specimen, it is not recommended that one utilize such high reinforcement ratios. In contrast, the specimen with a reinforcement ratio of  $2\rho_p$  carried nearly the same load, deflected more than twice as much as Specimen S300, and resisted twice as many loading cycles. It is therefore recommended that, for walls with an aspect ratio of 28, the maximum reinforcement ratio be limited to  $2\rho_p$ .

For the case of minimum reinforcement, the designer must keep in mind that, in general, narrow strips of composites are subjected to higher shear transfer stresses that could result in early delamination. It is recommended that one check these stresses and select the appropriate type of composite strip with adequate contact area to delay or eliminate this mode of failure.

## Calculation of Load and Deflection

The flexural capacity of the walls can be calculated using the linear elastic approach discussed earlier. The load corresponding to the three stages of the behavior can be determined with a fair degree of accuracy. The results of the study suggest that the average longitudinal tensile strain in the composite strips be limited to 0.004 for the first visible bed-joint crack, 0.0055 for the first delamination of the composite strip, and 0.01 for the ultimate failure. The calculation of these three loads, as shown in Fig. 9 and Table 2, can provide the designer with an overall estimation of the factors of safety relative to the applied service loads.

According to the experimental data, the deflection of the retrofitted walls can be calculated with the modified expressions presented in (4)–(6). These equations predict the cracking and delamination of the wall fairly accurately. However, the equations cannot be applied to predict the ultimate deflection of the wall because the maximum deflection is influenced by many factors, such as excessive delamination, cracking and softening of brickwork, and fracture of the composite strips among others.

For service conditions, it is recommended that one limit the maximum deflection to  $0.007h$  and the tensile strain in the composite strip to 0.004. The deflection limit represents <30% of the measured ultimate values, and it is always less than the deflection corresponding to the delamination of composite strips. The maximum span drift suggested for the service condition in URM beams is  $1/600$  (American 1995). Therefore, the proposed retrofit scheme allows an increase in the deflections of more than four times to  $0.007h$ .

As discussed previously, the strain limit of 0.004 corresponds to the load causing the first visible bed-joint crack. Test results indicate that this load is approximately 40% of the maximum pressure supported by the walls. Therefore, a sufficient factor of safety in load-carrying capacity is provided by this guideline. Similar limits on strain have been proposed for RC walls retrofitted with fiber composites (ICBO 1997).

## Fracture Ductility Index

One of the shortcomings of fiber composites is their inability to deform in an inelastic manner. This problem has been observed by many researchers in the case of concrete beams reinforced with composite tendons or reinforcing bars. The problem is of particular interest in this application as it is desired to have a ductile failure of the retrofitted walls.

Due to the lack of a yield point in composites, the use of the traditional definition of ductility is not warranted. However, in many applications, including the retrofitted walls discussed here, the presence of the composite strips does allow the walls to undergo significant deformation prior to failure. There is also energy dissipation through cracking and softening of the masonry and delamination of the composite strips. Instead of the traditional yield point as a reference, it is proposed that one consider the load corresponding to the first visible bed-joint crack.

A fracture ductility index ( $FD$ ) is proposed. The index is defined as the ratio of the deflection at pressures beyond that causing the first visible bed-joint crack to that corresponding to the first visible bed-joint crack. The fracture ductility index is defined mathematically as

$$FD = \frac{\delta_{max}}{\delta_{cr}} \quad (11)$$

Because the deflection corresponding to the cracking capacity is very small and difficult to detect, it was decided to use the deflection at the first visible bed-joint crack. Other researchers have also used the concept of the first visible crack to char-

acterize the cracking capacity of block masonry walls subjected to out-of plane load (Abboud et al. 1996).

A fracture ductility index as high as 5 was obtained in the test specimens (Table 1). Even Specimen S300 that failed prematurely by in-plane shear stresses exhibited a ductility index of 2. In steel RC or masonry members, ductility increases as the reinforcement ratio is reduced. This is because the lower reinforcement ratio results in larger steel strain and curvature at failure. However, due to the elastic behavior of composite strips, a similar trend cannot be obtained in URM walls retrofitted with composite materials. This is evident from the test results shown in Table 1, where regardless of the aspect ratio and the amount of reinforcement, the maximum recorded fracture ductility index was similar for all walls and it was limited to 5. Therefore, the data do not justify a reduction in the reinforcement ratio in an attempt to achieve a higher ductility index.

## CONCLUSIONS

The experimental results obtained from URM brick masonry walls retrofitted with glass-fiber composite strips are compared with respect to those obtained from analytical solutions. The analytical results were obtained using the beam theory through the ultimate strength and linear elastic approaches. Clearly, there are a number of issues that require further investigation. However, within the scope of this study, the following conclusions can be made:

- A linear elastic solution is recommended for evaluation of the flexural capacity of URM masonry walls retrofitted with composite materials. This procedure results in a lower calculated strength compared to the measured values for the recommended range of reinforcement ratios.
- The deflection of walls for various stages of loading can be calculated using the modified expressions in (4)–(6). It is recommended that this deflection be limited to  $0.007h$ .
- The average tensile strain in the composite strip for the three stages of loading is 0.004 for the first visible bed-joint crack, 0.0055 for the first delamination, and 0.01 for the ultimate condition. It is recommended that the maximum service load be limited to that corresponding to a strain of 0.004.
- The maximum reinforcement ratio as a multiple of the balanced reinforcement ratio is 0.4 and 2 for walls with aspect ratios of 14 and 28, respectively.
- The majority of the specimens exhibited a fracture ductility index of 3.75–5.0 regardless of the amount of reinforcement present.

## ACKNOWLEDGMENTS

Partial financial support for this study was provided under National Science Foundation, Washington, D.C., Grant No. CMS-9412950. Dr. S. C. Liu, program director, Velazquez-Dimas was supported through a scholarship provided by CONACYT and Universidad Autonoma de Sinaloa, Mexico. All support is gratefully acknowledged.

The views expressed in this paper are those of the writers and do not necessarily represent the views of the sponsors.

## APPENDIX I. REFERENCES

- Abboud, B. E., Hamid, A. A., and Harris, H. G. (1996). "Flexural behavior of reinforced concrete masonry walls under out-of-plane load." *ACI Struct. J.*, 93(3), 325–327.
- Abrams, D. P. (1996). "The return of masonry as a structural material." *Worldwide advances in structural concrete and masonry*, A. E. Schultz and S. L. McCabe, eds., 1–5.
- Abrams, D. P., Angel, R., and Uzarski (1993). "Transverse strength of damaged URM infills." *6th North Am. Masonry Conf.*
- American Concrete Institute (ACI)/ASCE/TMS Masonry Standards Joint

- Committee. (1995). "Building code requirements for masonry structures." *ACI 530-95/ASCE 5-95/TMS 402-95*
- Dawe, J. L., and Seah, C. K. (1989). "Out-of-plane resistance of concrete masonry infilled panels." *Can. J. Civ. Engrg.*, Ottawa, 16, 854–864.
- Ehsani, M. R., and Saadatmanesh, H. (1996). "Seismic retrofitting of URM walls with fiber composites." *The Masonry Soc. J.*, 14(2), 63–72.
- Ehsani, M. R., and Saadatmanesh, H. (1997). "Fiber composites: An economical alternative for retrofitting earthquake damaged precast-concrete walls." *Earthquake Spectra*, 13(2), 225–241.
- Ehsani, M. R., Saadatmanesh, H., and Velazquez-Dimas, J. I. (1999). "Behavior of retrofitted URM walls under simulated earthquake loading." *J. Comp. for Constr.*, ASCE, 3(3), 134–142.
- El-Badry, N. M. (1996). *Proc., 2nd Int. Conf. (ACMBS II), Advanced Compos. Mat. in Bridges and Struct.*, 1–1027
- ICBO Evaluation Services, Inc. (1997). *Acceptance criteria for concrete and reinforced and unreinforced masonry strengthening using fiber-reinforced composite systems ACI25-R2-0497 (BCGIBNH)*. International Conference of Building Officials, Whittier, Calif.
- International Conference of Building Officials (ICBO). (1991). *Uniform Building Code*. Whittier, Calif.
- Jones, R. M. (1975). *Mechanics of composite materials*. Scripta Book Co., Washington, D.C.
- Lizundia, B., Holmes, W. T., Longstreth, M., and Ken, A. (1997). *Development of procedures to enhance the performance of rehabilitated URM buildings, NIST GCR 97-724-1*. U.S. Department of Commerce, Washington, D.C.
- Mulenci, F. (1997). "Class notes for advanced composite materials." Dept. of Acrosp. and Mech. Engrg., University of Arizona, Tucson, Ariz.
- Marine, M. E. (1994). "Moment curvature and load-deflection behavior of plated R/C sections." *Master Rep.*, University of Arizona, Tucson, Ariz.
- Nanni, A. (1993). *Fiber-reinforced plastic (FRP) reinforced for concrete structures: Properties and applications*. Elsevier Science, New York.
- Saadatmanesh, H., and Ehsani, M. R. (1996). *Proc., 1st Int. Conf. on Compos. in Infrastruct.: Fiber Compos. in Infrastruct.*, 1–1231.
- Saadatmanesh, H., and Ehsani, M. R. (1998). *Proc., 2nd Int. Conf. on Compos. in Infrastruct.: Fiber Compos. in Infrastruct.*, Vols. I and II, 1–1506.
- Sinha, B. P. (1978). "A simplified ultimate load analysis of laterally loaded model orthotropic brickwork panels of low tensile strength." *The Struct. Engrg.*, London, 4(56B), 81–84.
- Sveinsson, B. I., Mayes, R. L., Kelly, T. E., and Jones, I. R. (1987). "Out-of-plane response of masonry walls to seismic loads." *Proc., 4th North Am. Masonry Conf.*, 46.1–46.10.
- Taerwe, L. (1995). "Non-metallic (FRP) reinforcement for concrete structures." *Proc., 2nd Int. RILEM Symp. (FRPRCS-2)*.
- Velazquez-Dimas, J. I. (1998). "Out-of-plane cyclic behavior of URM walls retrofitted with fiber composites." PhD dissertation, Dept. of Civ. Engrg. and Engrg. Mech., University of Arizona, Tucson, Ariz.

## APPENDIX II. NOTATION

The following symbols are used in this paper:

- $b_m$  = width of brick-beam section;  
 $C$  = compression mode of failure;  
 $C_m$  = compressive force of brick-beam section;  
 $D$  = delamination mode of failure;  
 $E_f$  = modulus of elasticity of composite strip;  
 $E_m$  = modulus of elasticity of brickwork;  
 $FD$  = fracture ductility index;  
 $f_f$  = stress in composite strip;  
 $f_m$  = stress in masonry;  
 $f_r$  = modulus of rupture;  
 $h$  = wall height;  
 $I_c$  = cracked moment of inertia;  
 $I_g$  = gross moment of inertia;  
 $kt$  = neutral axis position;  
 $M$  = flexural moment;  
 $M_c$  = flexural cracking moment;  
 $M_D$  = flexural moment at first delamination;  
 $M_{cr}$  = flexural moment at first visible bed-joint crack;  
 $P$  = applied pressure;  
 $P_{cr}$  = load corresponding to first visible bed-joint crack;  
 $P_D$  = load corresponding to first delamination;

$P_{max}$  = maximum supported pressure (psf);  
 $P_{ult}$  = load at failure;  
 $S$  = shear mode of failure;  
 $T$  = tension mode of failure;  
 $T_c$  = tensile force in composite strip;  
 $t$  = wall thickness;  
 $t_c$  = thickness of composite strip;  
 $W$  = width of composite strips;  
 $w$  = wall weight (psf/wythe);  
 $Z$  = lever arm between resultant forces;

$\delta$  = deflection at any load;  
 $\delta_{d1}$  = deflection at first delamination;  
 $\delta_{d2}$  = deflection at first visible bed-joint crack;  
 $\epsilon_{c1}$  = strain corresponding to first visible bed-joint crack;  
 $\epsilon_{c2}$  = strain corresponding to first delamination;  
 $\epsilon_c$  = strain in composite strip;  
 $\epsilon_m$  = strain in masonry;  
 $\epsilon_{ult}$  = strain corresponding to ultimate load;  
 $\rho$  = reinforcement ratio; and  
 $\rho_b$  = balanced reinforcement ratio.